

SPECTROELLIPSOMETRIC CHARACTERIZATION OF ION IMPLANTED SEMICONDUCTORS AND POROUS SILICON¹

T. Lohner², N.Q. Khanh

Research Institute for Technical Physics and Materials Science, H-1121 Budapest,
Konkoly Thege ut 29-33. HUNGARY

Zs. Zolnai

Department of Atomic Physics, Technical University of Budapest, Budapest,
Budafoki ut 8, Hungary

Received 16 July 1998, accepted 30 July 1998

In the past years spectroscopic ellipsometry (SE) was applied to materials science problems as an optical technique for non destructive depth profiling and characterization of multilayer structures and interfaces with considerable success. The measured optical response of the multicomponent and/or multilayer structure under investigation can only be related to actual material properties by a model calculation. The successful application of ellipsometry is not only determined by the quality of the measurements, but more importantly by the quality of the optical model. Several examples for the different application of SE are reviewed.

Two recent examples of multilayer analysis illustrate possibilities: in the first example damage created by ion implantation in single-crystalline silicon and in silicon carbide was characterized using ellipsometry and Rutherford Backscattering Spectrometry (RBS) in combination with channeling. In the second example electrochemically prepared porous silicon layers (PSL) were investigated by SE.

1 Introduction

The past years have seen widespread use of spectroscopic ellipsometry (SE) in different fields of research. Ellipsometry offers great promise for characterization, monitoring and control of a wide variety of processes, especially in microelectronics.

The requirement for the formation of very shallow junctions in silicon necessitates the application of high depth resolution analytical methods for the investigation of the depth distribution of implanted dopants and that of damage created by implantation.

¹Presented at The International Workshop on Diagnostics of Solid State Surfaces and Interfaces, Bratislava, 24 – 26 June 1998

²E-mail address: lohner@ra.atkiki.kfki.hu, lohner@mia.kfki.hu, Fax: (36-1) 395 9284

The properties of defects generated by ion irradiation determine the basic features of implantation-related processes such as ion beam induced layer-by-layer recrystallization and amorphization. SE is an established method for determination of damage depth profile generated by ion implantation [1-4]. Fukarek et al. investigated 250 eV and 10 keV boron implantation damage using in-situ single wavelength ellipsometric etch depth profiling and non-destructive variable angle of incidence SE [5].

It is of considerable interest to investigate the optical properties of amorphous semiconductors, one of the straightforward methods is SE [6]. Surface and interface phenomena were investigated also using SE [7]. Pinter and co-workers investigated nucleation and growth of MW-CVD diamond films using SE and ion beam analysis methods [8]. Tonova and Konova developed a new algorithm for ellipsometric depth profiling [9,10]. Lehnert et al. performed in situ characterisation of oxide and polycrystalline silicon layers at high temperatures using a spectroellipsometer integrated in a vertical LPCVD-batch furnace [11].

Dielectric function of bulk of 4H-SiC and 6H-SiC was determined by Zolner and Hilliker using spectroellipsometry. The ellipsometric angles from 0.72 eV to 6.6 eV were measured using a rotating analyzer ellipsometer with compensator. The compensator allows accurate measurements even for large gap materials [12].

Kryzanowska et al. investigated refractive index anisotropy of porous silicon layers with columnar structure using single wavelength ($\lambda = 632.8\text{nm}$) multiple angle of incidence ellipsometry [13]. The porosity of their samples was in the range 23% - 70%. Formulas for Fresnel refraction coefficients, corresponding to uniaxially anisotropic film on isotropic substrate, were applied to determine ordinary and extraordinary refractive indices of porous Si layers. They assumed that the values of extinction coefficients were negligible at this wavelength.

Fried et al. made systematic study on thin porous silicon layer of different porosities formed by electrochemical etching and followed by thermal oxidation and electrochemical oxidation. The oxidized and the non-oxidized PS layers were analyzed by spectroscopic ellipsometry, spectroscopic reflectometry and secondary mass spectrometry. [14]. Molnár et al. applied SE for the characterization of porous silicon layers fabricated for LED structures [15].

In the present work the ion bombardment induced damage was investigated in Ne implanted silicon and Al implanted SiC using SE and ion beam analysis. Thin porous silicon layers were characterized by SE to obtain porosity and layer thickness values.

2 Experimental

2.1 Ion implantation

To investigate damage profile 150 keV Ne⁺ were implanted at room temperature in (100) silicon. The implantation dose was 1×10^{15} atoms/cm². To reduce the possible effect of the native oxide layer the silicon substrates were etched in HF solution before inserting them into the implantation chamber. In addition, silicon substrates having usual native oxide layer were subjected to Ne implantation, too. In the case of SiC, 200 keV Al⁺ ions were implanted into 4H-SiC. RBS and channeling techniques with 2 MeV

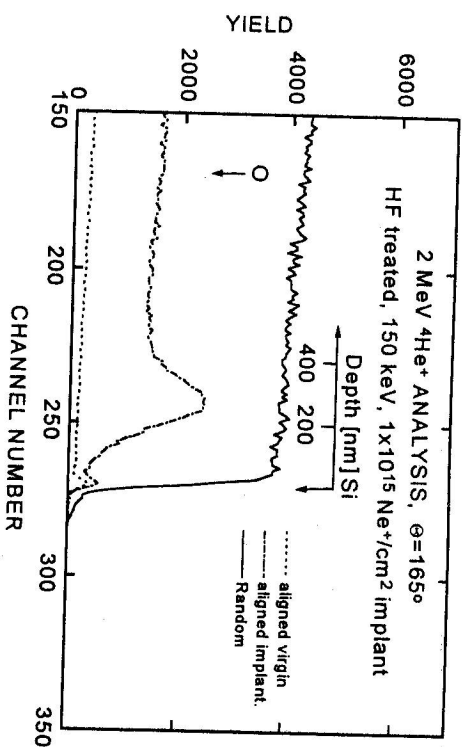


Fig. 1. RBS spectra recorded with a detector placed at scattering angle of 165°. For comparison, the spectrum measured on a virgin (unimplanted) silicon sample is also included.

and 3.5 MeV He⁺ ions were used in the experiments. To evaluate the spectra we used the RBX code written by Kótai [16], which can also handle channelled spectra.

2.2 Preparation of porous silicon layers

Porous silicon layer (PSL) formation was performed in an teflon anodisation cell having ohmic back contact and using HF/ethanol containing solution as an electrolyte. The specimen to be etched is placed at the anode while a Pt electrode is used as a cathode in a galvanostatic regime with constant current density in the range of 10 - 20 mA/cm². Local doping level and HF concentration of the electrolyte along with the applied current density determine the porosity obtainable. Ethanol addition to the electrolyte enhances the wettability and release of bubbles from the surface evolving during electrochemical reaction. Interference colours in the thickness range of interest go from yellow through gold and violet up to royal blue. Corresponding etching times range from 1 - 10 s depending on process parameters. PSL formation on top of an n⁺-p junction benefits from the hole injection obtained from the forward biased diode, thereby ensuring a lateral homogeneity.

2.3 Ellipsometry

In reflection ellipsometry the experimental result is given by:

$$\rho = R_p/R_s = \tan \Psi \exp(i\Delta)$$

where ρ is the complex reflectance ratio. R_p and R_s are the complex amplitude reflection coefficients for the parallel (p) and perpendicular (senkrecht, s) polarizations relative to the plane of incidence. $\tan \Psi$ is the intensity ratio and Δ is the relative phase

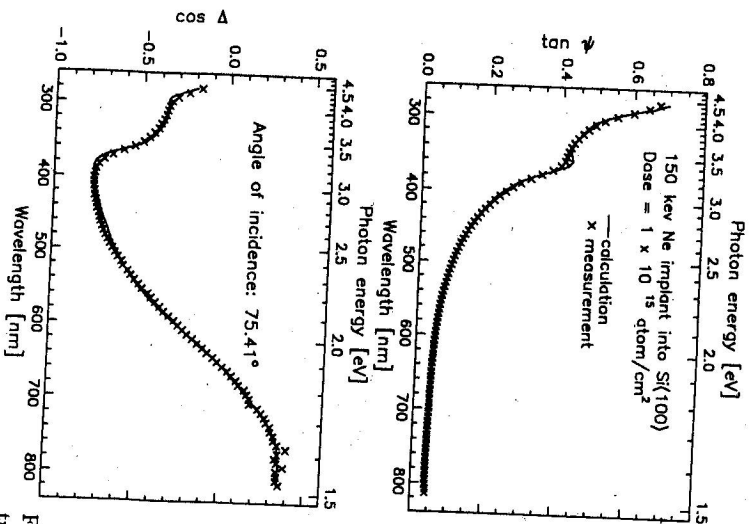


Fig. 2. Experimental and best fit SE spectra for 150 keV Ne implanted silicon

difference. With a rotating element ellipsometer one can determine $\tan \Psi$ and $\cos \Delta$. The SE spectra were measured with a rotating polarizer ellipsometer.

With reference to the work of Aspnes, Theeten, and Hotlier [17], the quantity used to describe the agreement between the experimental data and the spectrum calculated on basis of a selected optical model is defined as the unbiased estimator (σ):

$$\sigma = \frac{1}{2N - p - 1} \sqrt{\sum_{j=1}^N [(\cos \Delta_j^{\text{exp}} - \cos \Delta_j^{\text{calc}})^2 + (\tan \Psi_j^{\text{exp}} - \tan \Psi_j^{\text{calc}})^2]}$$

where N is the number of wavelengths and p is the number of fitted parameters.

Aspnes and his co-workers accept as valid, models with unbiased estimators ranging from 0.09 to 0.01 [17]. The unbiased estimator also serves to help limit the number of parameters that can be selected for a given model. In the modelling process, if the number of parameters increases, the unbiased estimator could decrease, increase or remain the same. If the unbiased estimator does not decrease, then the addition of the parameter for a given model, is rejected.

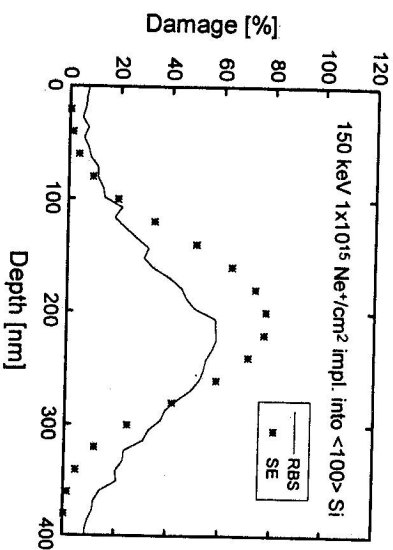


Fig. 3. Damage depth profiles for the 150 keV Ne implanted silicon sample extracted from ion beam analytical measurements (line) and from SE (*)

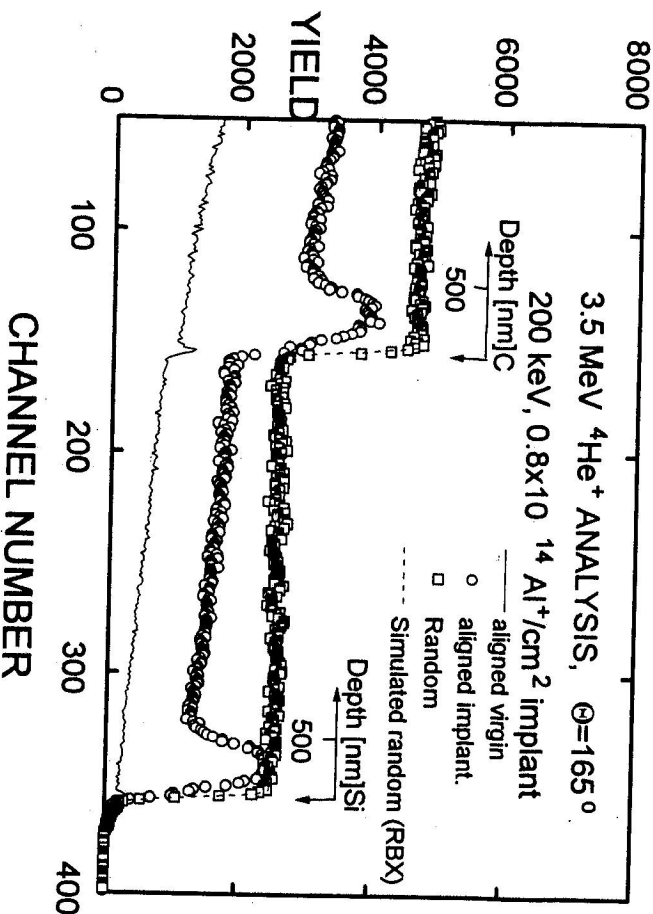


Fig. 4. Backscattering spectra of ion implanted 4H-SiC sample. For comparison, spectrum measured on not implanted (virgin) 4H-SiC sample also shown.

To get damage profile from SE data linear regression analysis (multiparameter fitting) was used. In several cases Monte Carlo search was applied to get the initial data set for iteration.

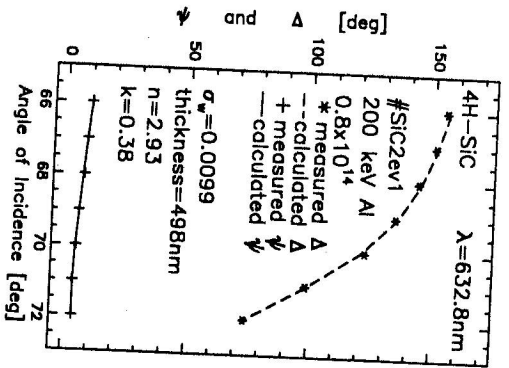


Fig. 5. The measured and calculated ellipsometric angles and versus the angle of incidence for the Al implanted 4H-SiC sample.

3 Results and discussion

Figure 1 presents the RBS spectra of α 's scattered through 155° for the Ne implanted sample that was HF etched prior to implantation. For comparison, the spectrum measured on a virgin (unimplanted) silicon sample is also included. In accordance with projected range calculations, a partially disordered region is observable around 250 nm depth.

For the evaluation of ellipsometric data of the 150 keV Ne implanted sample we used the optical model consisting of a native oxide layer, a thin totally amorphous layer, a slightly damaged transition layer, a partially amorphized region described by a damage profiles (with four independent parameters with two coupled half Gaussian shaped and two standard deviations), and single crystalline silicon substrate [18]. The complex refractive index of each layer (at each wavelength) is calculated from the actual damage level by the B-EMA using the complex dielectric function of c-Si and ion-implanted amorphous silicon (a-Si) [19]. Figure 2 shows the result of SE fitting together with experimental data for the 150 keV Ne implant.

Figure 3 compares the damage depth distribution extracted from channeling data and SE data, respectively. There is only a small deviation concerning the positions of the peaks, however, a larger deviation is observable concerning the height and the width of the distributions. The possible explanation might be that the optical modelling of the partially disordered region generated by bombarding with a relatively light mass ion as Ne by the mixture of ion implantation amorphized silicon and single crystalline silicon has certain limitations.

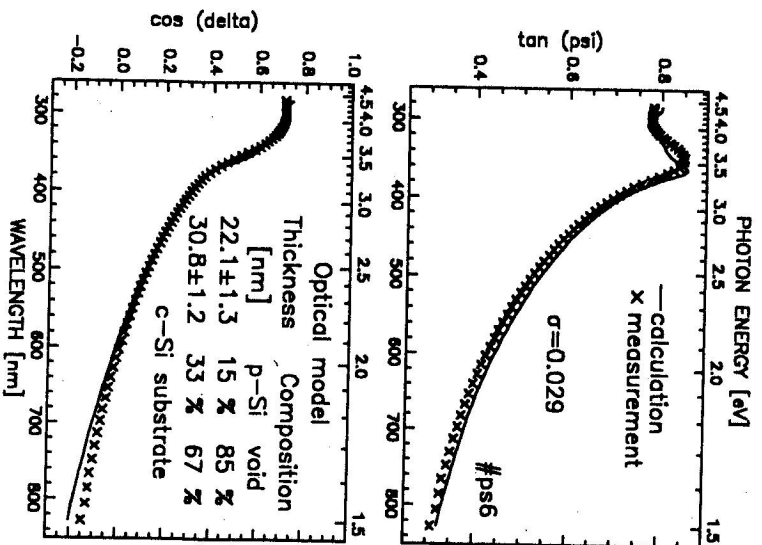


Fig. 6. Result of SE fitting together with experimental data for the thinnest PSL sample. The insert shows the optical model

Figure 4 shows the backscattering spectra of 200 keV Al implanted 4H-SiC sample. The energy of the analyzing He beam was adjusted to 3.5 MeV, at this energy the non Rutherford scattering cross section ensures an enhancement factor of approximately 6 for the carbon, in other words, this makes possible to obtain sufficiently high backscattering yield for carbon, too. The aligned spectrum taken on the implanted SiC sample shows a heavily but not completely damaged thin region near the surface.

Figure 5 illustrates the result of the single wavelength ellipsometric characterization: the measured as well as the calculated and values are shown versus the angle of incidence. For the evaluation the one layer model was applied, the refractive index, the extinction coefficient and the (average) thickness of the damaged layer were chosen as free parameters, the refractive index and the extinction coefficient of the substrate (single crystalline SiC) were taken from the literature [20]. The layer thickness values obtained using ion beam analytical measurement and ellipsometry are in rather good agreement, it is important to note that the evaluations for the two methods were really

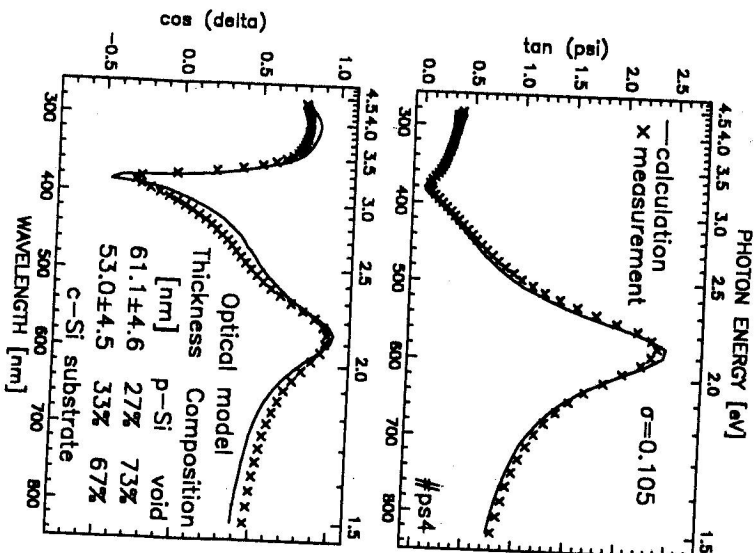


Fig. 7. Result of SE fitting together with experimental data for the thickest PSL sample. The inset shows the optical model.

independent.

In the experiment concerning the spectroellipsometric investigation of thin porous silicon a series of samples (ps6, ps5 ps1 and ps4) was prepared with the same nominal porosity, the etching time, i.e. the layer thickness was varied between nominally 50 and 120 nm choosing an anodization duration between 1s and 10 s.

For the analysis of SE data we used the conventional method of assuming an appropriate optical model and fitting the model parameters (layer thicknesses and volume fraction of the constituents in the layer) by linear regression.

The PSL was modelled first as a mixture of void and crystalline silicon, i.e. the complex refractive index of the layer was calculated by Bruggeman effective medium approximation using void and crystalline silicon as end-points. In the second optical model the PSL was considered as a mixture of void and fine-grain polycrystalline silicon. The dielectric function of the fine-grain polycrystalline silicon was taken from the work published by Jellison [21].

The spectrum corresponding to the thinnest layer is displayed in Fig. 6. The

Sample No	MAIE	Spectroellipsometry					
		One layer model c-Si + void		One Layer model p-Si + void			
	<i>t</i> [nm]	porosity[%]	<i>d</i> [nm]	σ	porosity[%]	<i>d</i> [nm]	σ
ps6	43	72	40	0.13	72	41	0.10
ps5	62	73	56	0.21	73	60	0.12
ps1	87	71	85	0.21	73	88	0.14
ps4	102	69	105	0.31	70	107	0.34

Table 1. Results of evaluation of ellipsometric measurements on porous silicon samples. The column labelled MAIE contains layer thickness values (*t*) extracted from the one-wavelength multiple-angle-of-incidence ellipsometric measurements. *d* and σ show the layer thickness values and unbiased estimator for the evaluation of spectroellipsometric data using the one layer models.

PSL was divided into two sublayers to obtain proper agreement between measured and simulated spectra describing a porosity gradient. Figure 7 presents the measured spectra of the thickest sample together with the results of multiparameter fitting.

Table 1 summarizes the layer thickness values resulting from the evaluation of one-wavelength multiple-angle-of-incidence ellipsometric measurements and SE measurements together with the porosity values and values of unbiased estimator characterizing the quality of the fit using one layer model. Comparing the results presented in Table 1 and in the Figures 6-7 one can observe a significant reduction in the values of unbiased estimator in the case of two layer optical model.

4 Conclusion

With proper optical modelling both single wavelength and spectroscopic ellipsometry as sensitive non-destructive non contact optical methods can be used for characterization of layers modified either using ion bombardment or electrochemical treatment.

Acknowledgment The authors would like to express their deep appreciation to I. Bársányi, P. Dexiák, M. Fried, J. Gyulai, W. Lehnert, M. Péter, P. Petrik, O. Polgár, É. Vázsonyi, and J. Waizinger for their contribution to this work. One of the authors (T.L.) is grateful to the organizers of the International Workshop on Diagnostics of Solid State Surfaces and Interfaces for inviting him to the Workshop.

This work was partially supported by OTKA grant No. TO25928 and by AKP grant No. 97-92 2,2.

References

- [1] P.J. McMarr, K. Vedam, J. Narayan: *J. Appl. Phys.* **59** (1986) 694
- [2] S. Lynch, M. Murtagh, G. M. Crean, P.V. Kelly, M. O'Connor, C. Jeynes: *Thin Solid Films* **233** (1993) 199

- [3] M. Fried, T. Lohner, W. A. M. Arnink, L. J. Hanekamp, A. van Silfhout: *J. Appl. Phys.* **71** (1992) 2835
- [4] M. Fried, T. Lohner, J. Gyulai: *Ellipsometric Analysis*, chapter 1, in vol. 46 of *Semiconductors and Semimetals: Effect of Disorder and Defects in Ion-Implanted Semiconductors: Optical and Photoemission Characterization*, eds. C. Christofides & G. Ghibaudo, 1997, Academic Press, San Diego, ISBN 0-12-752146-1 p. 1.
- [5] W. Fukarek, W. Müller, N. Hatzopoulos, D.G. Armour, J.A. van den Berg: *Nuclear Instruments and Methods in Physics Research B* **127/128** (1997) 879
- [6] M. Fried, A. van Silfhout: *Physical Review B* **49** (1994) 5699
- [7] M. Gartner, C. Parlog, C. Ghita, A. Andrei, A. Ivan: *SPIE Vol.* **2461** p. 149.
- [8] I. Pinter, P. Petrik, E. Szilagyi, Sz. Kátai, P. Deák: *Diamond and Related Materials* **6** (1997) 1633
- [9] D. A. Tonova: *Optics Communications* **105** (1994) 104
- [10] D. Tonova, A. Konova: *Surface Science* **293** (1996) 195
- [11] W. Lehnert, P. Petrik, C. Schneider, L. Pfitzner, H. Ryssel: *Proceedings of the ULST Conference at NIST*, March 1998, Washington, in press
- [12] S. Zolner, J. N. Hilliker: *phys. stat sol (a)* **166** (1998) R9
- [13] H. Kryzanowska, M. Kullik, J. Zuk: *Proceedings of the European Materials Research Society Spring Meeting; Symposium B, Light Emission from Silicon: Progress Towards Si-based Optoelectronics*, to be published
- [14] M. Fried, O. Polgar, T. Lohner, S. Strehlke, C. Levy-Clement: *Proceedings of the European Materials Research Society Spring Meeting; Symposium B, Light Emission from Silicon: Progress Towards Si-based Optoelectronics*, to be published
- [15] K. Molnar, T. Mohácsy, P. Varga, E. Vásonyi, I. Bárony: *Proceedings of the European Materials Research Society Spring Meeting; Symposium B, Light Emission from Silicon: Progress Towards Si-based Optoelectronics*, to be published
- [16] E. Kótai: *Nucl. Instr. Meth.* **B 85** (1994) 588
- [17] D. E. Aspnes, J. B. Theeten, F. Hottier: *Phys. Rev. B* **20** (1979) 3292
- [18] M. Fried, T. Lohner, W. A. Arnink, L. J. Hanekamp, A. van Silfhout: *J. Appl. Phys.* **71** (1992) 2835
- [19] M. Fried, T. Lohner, W. A. M. Arnink, L. J. Hanekamp, A. van Silfhout: *J. Appl. Phys.* **71** (1992) 5260
- [20] P.T.B. Schaffer: *Appl. Opt.* **62** (1972) 1034
- [21] G.E. Jellison, Jr., M.F. Chisholm, S.M. Gorbalkin: *Appl. Phys. Lett.* **62** (1993) 3348